



Hydroxylated chalcones with dual properties: Xanthine oxidase inhibitors and radical scavengers



Emily Hofmann^a, Jonathan Webster^a, Thuy Do^a, Reid Kline^a, Lindsey Snider^a, Quintin Hauser^a, Grace Higginbottom^b, Austin Campbell^b, Lili Ma^a, Stefan Paula^{a,b,c,*}

^a Department of Chemistry, Natural Sciences Center, Northern Kentucky University, Highland Heights, KY 41099-1905, USA

^b Department of Chemistry, Purdue University, 560 Oval Drive, West Lafayette, IN 47907-2084, USA

^c Department of Biochemistry, Purdue University, 175 South University Street, West Lafayette, IN 47907-2063, USA

ARTICLE INFO

Article history:

Received 19 October 2015

Revised 6 December 2015

Accepted 14 December 2015

Available online 17 December 2015

Keywords:

Xanthine oxidase

Chalcones

Enzyme inhibition

Radical scavenging

Anti-oxidants

Reperfusion injuries

Caffeic acid

Reactive oxygen species

Cell viability

ABSTRACT

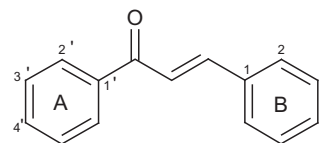
In this study, we evaluated the abilities of a series of chalcones to inhibit the activity of the enzyme xanthine oxidase (XO) and to scavenge radicals. 20 mono- and polyhydroxylated chalcone derivatives were synthesized by Claisen–Schmidt condensation reactions and then tested for inhibitory potency against XO, a known generator of reactive oxygen species (ROS). In parallel, the ability of the synthesized chalcones to scavenge a stable radical was determined. Structure–activity relationship analysis in conjunction with molecular docking indicated that the most active XO inhibitors carried a minimum of three hydroxyl groups. Moreover, the most effective radical scavengers had two neighboring hydroxyl groups on at least one of the two phenyl rings. Since it has been proposed previously that XO inhibition and radical scavenging could be useful properties for reduction of ROS-levels in tissue, we determined the chalcones' effects to rescue neurons subjected to ROS-induced stress created by the addition of β -amyloid peptide. Best protection was provided by chalcones that combined good inhibitory potency with high radical scavenging ability in a single molecule, an observation that points to a potential therapeutic value of this compound class.

© 2015 Elsevier Ltd. All rights reserved.

1. Introduction

Chalcones are natural products with a broad range of bioactivities that are widely found in the plant kingdom.^{1,2} Structurally, they consist of two aryl groups (A- and B-rings) connected by an α,β -unsaturated ketone moiety that typically assumes the thermodynamically more stable *E* configuration (Scheme 1). Whereas the aryl groups can carry a variety of substituents, hydroxyl, methoxy, and alkenyl groups are by far the most commonly encountered ones in nature. Because of their structural simplicity and the associated ease of synthesis, chalcones continue to enjoy considerable attention from medicinal chemists exploring new molecular scaffolds for the design of novel therapeutics.^{3–5} Amongst the numerous bioac-

tivities of chalcones are anticancer and antiviral activities, but they also are known to possess radical scavenging properties and inhibitory potency against the enzyme xanthine oxidase (XO). The latter two properties make chalcones interesting candidates for the development of novel agents for the treatment of hyperuricemia or the suppression of oxidatively generated stress in tissue.



Scheme 1. The chalcone scaffold.

Abbreviations: A β , β -amyloid peptide; CAPE, caffeic acid phenethyl ester; DMF, dimethylformamide; DPPH, 2,2-diphenyl-1-picrylhydrazyl; EGTA, ethylene glycol tetraacetic acid; HRMS, high resolution mass spectrometry; MOMO, methoxymethoxy; MTT, 3-(4,5-dimethylthiazol-2-yl)-2,5-diphenyltetrazolium bromide; NADPH, nicotinamide adenine dinucleotide; PBS, phosphate-buffered saline; ROS, reactive oxygen species; XO, xanthine oxidase.

* Corresponding author. Tel.: +1 765 494 4378; fax: +1 765 494 0239.

E-mail address: Paulas@purdue.edu (S. Paula).

<http://dx.doi.org/10.1016/j.bmc.2015.12.024>

0968-0896/© 2015 Elsevier Ltd. All rights reserved.

For decades, XO inhibitors have been used for therapy of hyperuricemia, a condition associated with elevated levels of uric acid in the blood. Hyperuricemia has been linked to cardiovascular and chronic kidney disease and is also known to cause gout,^{6,7} the result of deposition of uric acid crystals in joints that trigger

inflammatory arthritis.⁸ Therapeutically used XO inhibitors suppress the production of uric acid, allowing for renal excretion of the uric acid precursors xanthine and hypoxanthine prior to the formation of uric acid. Allopurinol, a purine analog and prototype XO inhibitor which has been in use since 1966, is efficacious, but its relatively low potency (IC_{50} : 0.2–50 μM ⁶) requires dosages that can cause undesirable side effects, ranging from mild gastrointestinal upset to more severe hypersensitivity reactions and renal toxicity.^{9–12} Even though a number of promising alternative treatments of hyperuricemia such as recombinant uricase therapy, the use of interleukin-1 inhibitors, or the targeting of renal urate transporters are currently explored,^{13–15} XO inhibitors still remain first-line therapy. As the approval of the high-potency (subnanomolar range¹⁶), non-purine XO inhibitor febuxostat in 2009 shows,¹⁷ the development of new XO inhibitors based on novel structural scaffolds, including that of chalcones, continues to be an active field of current research.^{18,15}

In addition to their traditional use for the treatment of hyperuricemia, XO inhibitors have been proposed to be useful for the suppression of oxidatively generated stress in tissue, a condition caused by an imbalance between the production and removal rates of reactive oxygen species (ROS).^{19–21} In general, the term ROS denotes oxygen radicals, such as the superoxide anion radical, the hydroxyl radical, the peroxy radical, or the hydroperoxy radical, but it also applies to non-radical species that can convert into radicals, including hydrogen peroxide, hypochlorous acid, or ozone.²² Elevated ROS levels inside cells are toxic and cause damage by breaking down biopolymers. Oxidatively generated stress has been implicated in a number of diseases, among them cancer, neuropathy, inflammatory diseases, and reperfusion injuries.^{23–26} The latter can occur after surgery or ischemic events, such as heart attacks and strokes, once the blood circulation to oxygen-deprived tissue has been restored. The causes of reperfusion injuries are multi-faceted and factors like inflammation or the production of ROS are believed to be involved.^{27–30} At present, no approved pharmacological treatment of the damaging effects of ROS is available, but the development of compounds with anti-oxidative properties has been proposed to overcome this shortcoming.^{19–21} In order to rectify the imbalance between ROS production and removal rates, a suitable compound should prevent the generation of ROS by inhibiting XO, one of the well-known contributors to ROS production that generates the long-lived ROS species hydrogen peroxide and the superoxide radical anion. The effectiveness and versatility of such a XO inhibitor would be substantially enhanced if it were also able to scavenge some of the more stable ROS (from sources other than XO) before these convert into highly reactive and thus more damaging species, such as the hydroxyl radical. Although these two properties have been investigated separately for several compound classes, only a limited number of studies have characterized both properties for the same molecule.

Certain chalcones are known to inhibit XO and—unlike most other XO inhibitors including allopurinol and febuxostat—to act as radical scavengers. Even though these two properties have been appreciated for quite some time, no systematic efforts have been undertaken to date to exploit them for the development of medicinally useful agents for the reduction of ROS levels in tissue. For instance, no comprehensive structure–activity relationships (SAR) for chalcone-mediated XO inhibition have been established since most published studies focused in detail on the *in vitro* and/or *in vivo* properties of single molecules.^{31–35} In contrast, more information is available for the radical scavenging ability of chalcones, but without connecting this information with inhibitory potency, the goal of obtaining molecules with dual properties remains elusive. As proof-of-principle, such dual property agents have been described for several non-chalcone molecular scaffolds, among them coumarins or analogs of caffeic acid.^{19–21,36} Finally, the

potential medicinal value of one of these compounds, caffeic acid phenethyl ester (CAPE), has been demonstrated in animal studies that showed protective effects against ischemia-induced reperfusion injuries in brain and muscle tissues of rodents.^{37–39}

Chalcones can be synthesized in a relatively straightforward manner, often by acid- or base-catalyzed Claisen–Schmidt condensation of aryl aldehydes and ketones under homogeneous or heterogeneous conditions. Typical acid catalysts are $AlCl_3$, $RuCl_3$, silica- H_2SO_4 , and TiO_2/SO_4^{2-} ^{40,41} whereas frequently used base catalysts include KOH , $NaOH$, K_2CO_3 , $Ba(OH)_2$, and MgO .⁴² Heterogeneous Claisen–Schmidt condensation reactions are usually assisted by microwave⁴³ or ultrasound irradiation⁴⁴ to accelerate reaction rates or make the process environmentally more friendly. Recent reports have identified additional reactions that provide access to the chalcone scaffold, like the oxidation of alcohols⁴⁵, Meyer–Schuster rearrangement of propargylic alcohols,⁴⁶ and palladium-catalyzed carbonylative Heck reactions.⁴⁷ However, due to its convenient procedure, broad substrate scope, and high efficiency, the Claisen–Schmidt condensation method remains the most attractive choice for the synthesis of chalcones.

As a first step towards designing XO inhibitors with dual properties, we here report on our efforts to generate basic structure–activity relationship information on XO inhibition and radical scavenging mediated by hydroxylated chalcones. We first synthesized a selection of 20 chalcones that varied in number and position of hydroxyl groups at the two phenyl rings (Fig. 1). Next, we measured their inhibitory potencies against XO activity and their ability to scavenge the stable radical 2,2-diphenyl-1-picrylhydrazyl (DPPH), a species that is routinely used as a model for long-lived radicals. Experimental work was complemented by computational docking to elucidate and visualize crucial interactions between chalcone inhibitors and their target, XO. Lastly, we conducted cell-based viability assays to determine if the most active chalcones were able to help neurons cope with stress caused by elevated ROS levels generated artificially by addition of β -amyloid peptide ($A\beta$). Neurons were chosen for this assay because this cell-type would potentially suffer from reperfusion injuries after a stroke. The information obtained in this study can serve as the foundation for future projects aimed at further modifying and refining the properties of chalcones with the ultimate goal of developing this compound class into medicinally useful agents.

2. Experimental

2.1. Synthetic chemistry

With the exceptions of 2',5'-dihydroxyacetophenone which was obtained from Thermo Fisher Scientific (Waltham, MA) and 3,4'-dihydroxyacetophenone which was purchased from Matrix Scientific (Columbia, SC), all reagents and solvents were received from Sigma/Aldrich (St. Louis, MO) and used without further purification unless otherwise noted. For thin-layer chromatography, pre-coated Whatman silica gel F254 plates (GE Healthcare Bio-Sciences, Pittsburgh, PA) were used. Column chromatography was performed using pre-packed RediSep Rf Silica columns on a CombiFlash Rf flash chromatography system (Teledyne Isco, Lincoln, NE). NMR spectra were obtained using a Joel 500 MHz spectrometer (Peabody, PA). Chemical shifts were reported in parts per million (ppm) relative to the tetramethylsilane signal at 0.00 ppm. Coupling constants (J) were reported in Hertz (Hz). The peak patterns were indicated as follows: s, singlet; d, doublet; t, triplet; dt, doublet of triplet; dd, doublet of doublet; m, multiplet; q, quartet. High resolution mass spectra (HRMS) were recorded on a Micromass Q-TOF 2 (Waters, Milford, MA) or a Thermo Scientific LTQ-FTTM mass spectrometer (Waltham, MA) operating in the electrospray mode.

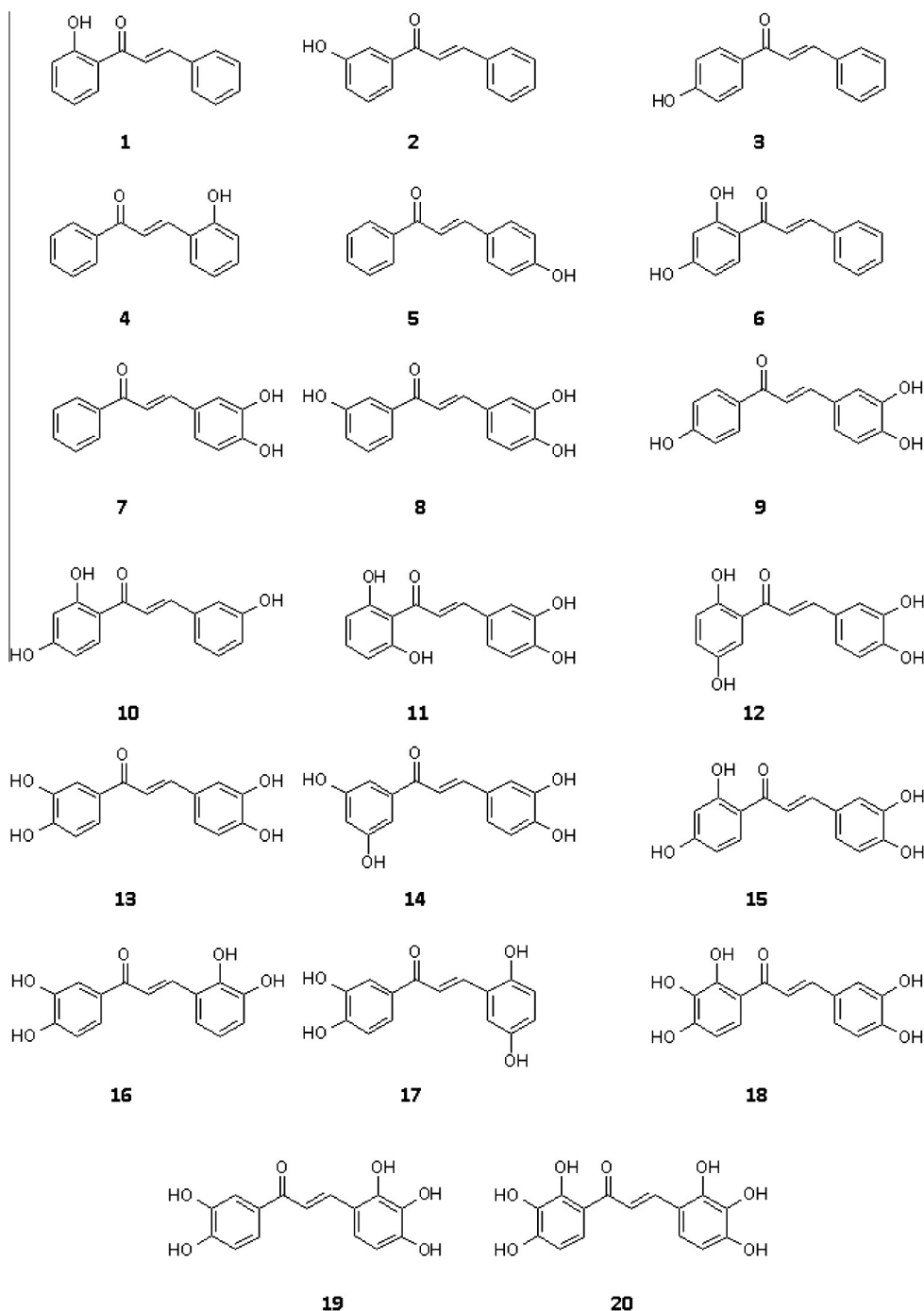


Figure 1. Chemical structures of chalcones synthesized and evaluated in bioassays.

2.1.1. General procedure for the synthesis of chalcones 1–5

As outlined in Figure 2, an aqueous solution of KOH (20% w/v, 2 mL) was added to a stirred solution of the appropriate acetophenone (1 mmol, 1 equiv) in ethanol (2 mL). The mixture was stirred at room temperature for 10 min. After complete dissolution, aryl aldehyde (1 mmol, 1 equiv) was added slowly and the reaction mixture was then stirred at room temperature for 24–72 h. After completion, the mixture was cooled to 0 °C on an ice bath and acidified with HCl (10% v/v aqueous solution). In most cases, the products precipitated out upon acidification with HCl. The crude product was filtered and further purified by recrystallization from ethanol. In the cases in which no precipitate formed, the mixture

was extracted with ethyl acetate and washed with brine and water. After drying over Na₂SO₄, the solvent was removed by rotary evaporation to give the crude product which was further purified by either recrystallization or automated medium performance liquid chromatography, eluting with an ethyl acetate/hexanes gradient (0–60%).

2.1.2. General procedure for the synthesis of chalcones 6–20

2.1.2.1. Methoxymethoxy (MOMO) protection. In a 100 mL oven-dried round bottom flask under argon protection, hydroxyaldehyde or acetophenone (10 mmol, 1 equiv) and 60 mL extra dry acetone were combined. After complete dissolution, the

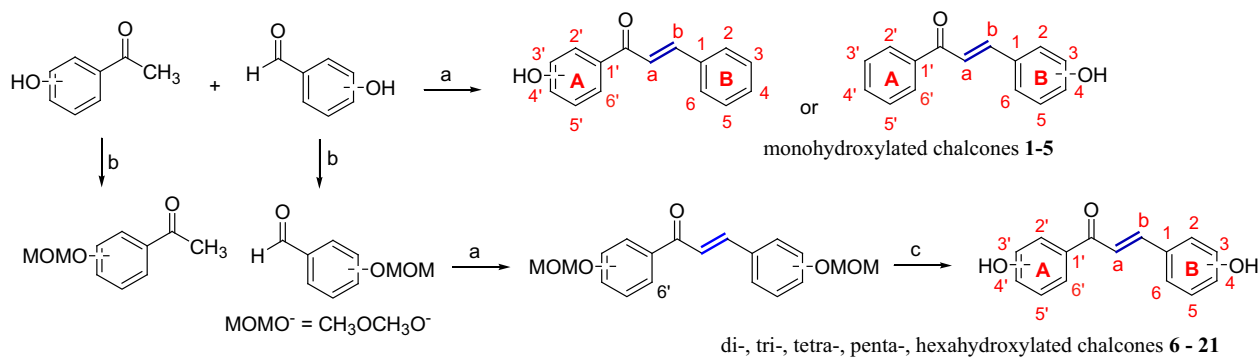


Figure 2. Synthesis of chalcones. Reaction conditions: (a) 20% KOH, EtOH, room temperature, 24–72 h; (b) CH₃OCH₂Cl, K₂CO₃, acetone, reflux, 4 h; (c) 10% HCl, EtOH, reflux, 15 min.

solution was cooled in an ice bath for 10 min and then K₂CO₃ (100 mmol, 10 equiv) was added. While stirring, methoxymethyl chloride (50 mmol, 5 equiv) was added dropwise. The mixture was first stirred at 0 °C for 30 min and then at under reflux conditions for 4 h. The mixture was cooled to room temperature and salts were removed by suction filtration. The solvent was removed by rotary evaporation to obtain the crude product which was further purified by automated medium performance liquid chromatography eluting with an ethyl acetate/hexanes gradient (0–20%).

2.1.2.2. Claisen–Schmidt condensation. To a stirred solution of the appropriate MOMO-protected acetophenone (1 mmol, 1 equiv) in ethanol (2 mL), an aqueous solution of KOH (20% w/v, 2 mL) was added. The mixture was stirred at room temperature for 10 min. After complete dissolution, the appropriate MOMO-protected aryl aldehyde (1 equiv) was added slowly and the reaction mixture was then stirred at room temperature for 24–72 h. After completion, the reaction mixture was cooled to 0 °C on an ice bath and acidified with HCl (10% v/v aqueous solution). In most cases, the products precipitated out upon acidification with HCl. The crude product was filtered and further purified by recrystallization from ethanol. In the cases in which no precipitate formed, the mixture was extracted with ethyl acetate and washed with brine and water. After drying over Na₂SO₄, the solvent was evaporated to give the crude product. The crude product was further purified by either recrystallization or automated medium performance liquid chromatography eluting with an ethyl acetate/hexanes gradient (0–60%).

2.1.2.3. MOMO deprotection. MOMO-protected chalcones (1 mmol) were added to ethanol (8 mL), followed by dropwise addition of HCl (10% aqueous solution, 3.5 mL). The mixture was heated under reflux conditions for 15 min. After cooling down to room temperature, the mixture was diluted with water (20 mL) and extracted with ethyl acetate three times (10 mL each). After drying over MgSO₄, filtration and evaporation of organic solvents, the product was obtained in good purity (Fig. 2).

2.1.2.3.1. (*E*)-1-(2-Hydroxyphenyl)-3-phenylprop-2-en-1-one (1)⁴⁸. Synthesized according to the aldol condensation general procedure described above. *R_f* = 0.70 (10% EtOAc/Hex). Yield: 26.7%. ¹H NMR (CDCl₃, 500 MHz, ppm): δ 7.93 (1H, d, *J* = 15.6 Hz), 7.94–7.92 (1H, m), 7.67 (1H, d, *J* = 16.1 Hz), 7.68–7.66 (2H, m), 7.50 (1H, t, *J* = 8.7 Hz), 7.45–7.43 (3H, m), 7.03 (1H, d, *J* = 8.7 Hz), 6.95 (1H, t, *J* = 7.4 Hz). ¹³C NMR (CDCl₃, 125 MHz, ppm): δ 193.8, 163.7, 145.6, 136.5, 134.7, 131.0, 129.8, 129.1, 128.8, 120.3, 120.1, 118.9, 118.7. HRMS: Calculated for C₁₅H₁₂O₂Na [M⁺Na] 247.0735, found 247.0728.

2.1.2.3.2. (*E*)-1-(3-Hydroxyphenyl)-3-phenylprop-2-en-1-one (2)⁴⁹. Synthesized according to the aldol condensation general procedure described above. Yellow solid. *R_f* = 0.75 (10% EtOAc/

Hex). Yield: 40.7%. ¹H NMR (CDCl₃, 500 MHz, ppm): δ 7.82 (1H, d, *J* = 15.6 Hz), 7.68 (1H, s), 7.62–7.61 (2H, m), 7.57 (1H, d, *J* = 7.8 Hz), 7.51 (1H, d, *J* = 15.6 Hz), 7.41–7.40 (3H, m), 7.37 (1H, t, *J* = 7.8 Hz), 7.14 (1H, d, *J* = 7.8 Hz). ¹³C NMR (CDCl₃, 125 MHz, ppm): δ 190.9, 156.7, 145.7, 139.5, 134.8, 130.9, 130.0, 129.1, 128.7, 122.0, 121.0, 120.7, 115.4. HRMS: Calculated for C₁₅H₁₂O₂Na [M⁺Na] 247.0735, found 247.0735.

2.1.2.3.3. (*E*)-1-(4-Hydroxyphenyl)-3-phenylprop-2-en-1-one (3)⁵⁰. Synthesized according to the general aldol condensation procedure described above. Yellow solid. Yield: 93.9%. ¹H NMR (acetone-*d*₆, 500 MHz, ppm): δ 9.29 (1H, br s), 8.09 (2H, d, *J* = 8.2 Hz), 7.86 (1H, d, *J* = 16.0 Hz), 7.81 (2H, d, *J* = 7.8 Hz), 7.74 (1H, d, *J* = 15.6 Hz), 7.46–7.42 (3H, m), 6.97 (2H, d, *J* = 8.2 Hz). ¹³C NMR (acetone-*d*₆, 125 MHz, ppm): δ 187.3, 162.0, 142.9, 135.5, 131.1, 130.4, 130.2, 129.0, 128.5, 122.1, 115.4. HRMS: Calculated for C₁₅H₁₂O₂Na [M⁺Na] 247.0735, found 247.0733.

2.1.2.3.4. (*E*)-3-(2-Hydroxyphenyl)-1-phenylprop-2-en-1-one (4)⁵¹. Synthesized according to the general aldol condensation procedure described above. Yellow solid. Yield: 26.2%. ¹H NMR (acetone-*d*₆, 500 MHz, ppm): δ 8.18 (1H, d, *J* = 16.0 Hz), 8.12–8.09 (2H, m), 7.88 (1H, d, *J* = 16.0 Hz), 7.82 (1H, t, *J* = 7.3 Hz), 7.65–7.55 (3H, m), 7.28 (1H, d, *J* = 7.3 Hz), 7.01 (1H, t, *J* = 6.9 Hz), 6.92 (1H, d, *J* = 6.4 Hz). ¹³C NMR (acetone-*d*₆, 125 MHz, ppm): δ 205.4, 157.1, 139.7, 138.7, 132.6, 131.8, 129.0, 128.7, 128.4, 122.2, 121.7, 120.1, 116.3. HRMS: Calculated for C₁₅H₁₂O₂Na [M⁺Na] 247.0735, found 247.0733.

2.1.2.3.5. (*E*)-3-(4-Hydroxyphenyl)-1-phenylprop-2-en-1-one (5)⁵¹. Synthesized according to the aldol condensation general procedure described above. Yellow solid. Yield: 76.2%. ¹H NMR (acetone-*d*₆, 500 MHz, ppm): δ 8.11 (2H, d, *J* = 8.2 Hz), 7.76–7.52 (7H, m), 6.92 (2H, d, *J* = 8.7 Hz). ¹³C NMR (acetone-*d*₆, 125 MHz, ppm): δ 205.4, 160.1, 144.4, 138.7, 132.5, 130.7, 128.6, 128.3, 126.8, 118.9, 116.0. HRMS: Calculated for C₁₅H₁₂O₂Na [M⁺Na] 247.0735, found 247.0737.

2.1.2.3.6. (*E*)-1-(2,4-Dihydroxyphenyl)-3-phenylprop-2-en-1-one (6)⁵². Synthesized according to the MOMO protection, aldol condensation, and general MOMO deprotection procedure described above. Yellow solid. *R_f* = 0.61 (30% EtOAc/Hex). Yield: 47.8%. ¹H NMR (acetone-*d*₆, 500 MHz, ppm): δ 8.12 (1H, d, *J* = 8.7 Hz), 7.92–7.79 (4H, m), 7.43–7.41 (3H, m), 6.51 (1H, d, *J* = 8.7 Hz), 6.42 (1H, s). ¹³C NMR (acetone-*d*₆, 125 MHz, ppm): δ 206.1, 166.5, 164.9, 143.9, 135.1, 132.8, 130.6, 129.0, 128.8, 120.9, 113.7, 108.1, 103.0. HRMS: Calculated for C₁₅H₁₂O₃Na [M⁺Na] 263.0684, found 263.0695.

2.1.2.3.7. (*E*)-3-(3,4-Dihydroxyphenyl)-1-phenylprop-2-en-1-one (7). Synthesized according to the MOMO protection, aldol condensation, and general MOMO deprotection procedure described above. Yellow solid. Yield: 47.8%. ¹H NMR (acetone-*d*₆, 500 MHz, ppm): δ 8.42 (1H, br s), 8.10 (2H, d, *J* = 7.8 Hz), 7.70–7.53 (5H, m), 7.33 (1H, s), 7.20 (1H, d, *J* = 8.3 Hz), 6.90 (1H, d, *J* = 8.3 Hz),

3.06 (1H, br s). ^{13}C NMR (acetone- d_6 , 125 MHz, ppm): δ 205.5, 148.2, 145.6, 144.8, 138.7, 132.5, 128.6, 128.3, 127.5, 122.4, 119.1, 115.6, 115.0. HRMS: Calculated for $\text{C}_{15}\text{H}_{12}\text{O}_3\text{Na}$ [M^+Na] 263.0678, found 263.0678.

2.1.2.3.8. (*E*)-3-(3,4-Dihydroxyphenyl)-1-(3-hydroxyphenyl)prop-2-en-1-one (**8**). Synthesized according to the MOMO protection, aldol condensation, and general MOMO deprotection procedure described above. Dark green solid. $R_f = 0.36$ (5% $\text{CH}_3\text{OH}/\text{CH}_2\text{Cl}_2$). Yield: 71.4%. ^1H NMR (acetone- d_6 , 500 MHz, ppm): δ 7.65 (1H, d, $J = 15.6$ Hz), 7.60 (1H, d, $J = 7.3$ Hz), 7.54 (1H, d, $J = 15.6$ Hz), 7.52 (1H, s), 7.36 (1H, t, $J = 7.8$ Hz), 7.32 (1H, s), 7.19 (1H, d, $J = 7.8$ Hz), 7.08 (1H, d, $J = 7.8$ Hz), 6.90 (1H, d, $J = 8.2$ Hz). ^{13}C NMR (CDCl_3 , 125 MHz, ppm): δ 189.0, 157.8, 148.2, 145.5, 144.6, 140.3, 129.8, 127.5, 122.4, 119.8, 119.7, 119.2, 115.6, 114.9, 114.8. HRMS: Calculated for $\text{C}_{15}\text{H}_{12}\text{O}_4\text{Na}$ [M^+Na] 279.0633, found 279.0642.

2.1.2.3.9. (*E*)-3-(3,4-Dihydroxyphenyl)-1-(4-hydroxyphenyl)prop-2-en-1-one (**9**). Synthesized according to the MOMO protection, aldol condensation, and MOMO deprotection general procedure described above. Dark green solid. $R_f = 0.48$ (30% EtOAc/Hex). Yield: 88.0%. ^1H NMR (acetone- d_6 , 500 MHz, ppm): δ 9.20 (1H, s), 8.56 (1H, s), 8.16 (1H, s), 8.06 (2H, d, $J = 8.2$ Hz), 7.62 (2H, s), 7.30 (1H, s), 7.17 (1H, d, $J = 7.8$ Hz), 6.95 (2H, d, $J = 8.7$ Hz), 6.88 (1H, d, $J = 7.8$ Hz). ^{13}C NMR (acetone- d_6 , 125 MHz, ppm): δ 187.2, 161.7, 147.9, 145.5, 143.6, 130.9, 127.7, 122.1, 119.0, 115.6, 115.3, 114.9. HRMS: Calculated for $\text{C}_{15}\text{H}_{12}\text{O}_4\text{Na}$ [M^+Na] 279.0633, found 279.0641.

2.1.2.3.10. (*E*)-1-(2,4-Dihydroxyphenyl)-3-(3-hydroxyphenyl)prop-2-en-1-one (**10**)⁵³. Synthesized according to the MOMO protection, aldol condensation, and MOMO deprotection general procedure described above. Orange solid. $R_f = 0.50$ (30% EtOAc/Hex). Yield: 59.5%. ^1H NMR (acetone- d_6 , 500 MHz, ppm): δ 8.14 (1H, d, $J = 8.7$ Hz), 7.88–7.77 (2H, m), 7.31–7.26 (3H, m), 6.94 (1H, d, $J = 7.8$ Hz), 6.47 (1H, d, $J = 8.7$ Hz), 6.37 (1H, s). ^{13}C NMR (acetone- d_6 , 125 MHz, ppm): δ 192.0, 166.9, 165.1, 157.9, 144.2, 136.5, 132.8, 130.1, 120.8, 120.3, 117.8, 115.3, 113.7, 108.1, 103.0. HRMS: Calculated for $\text{C}_{15}\text{H}_{12}\text{O}_4\text{Na}$ [M^+Na] 279.0633, found 279.0630.

2.1.2.3.11. (*E*)-1-(2,6-Dihydroxyphenyl)-3-(3,4-dihydroxyphenyl)prop-2-en-1-one (**11**). Synthesized according to the MOMO protection, aldol condensation, and MOMO deprotection general procedure described above. Orange solid. Yield: 88.6%. ^1H NMR (acetone- d_6 , 500 MHz, ppm): δ 8.64 (1H, s), 8.30 (1H, s), 8.05 (1H, d, $J = 15.6$ Hz), 7.76 (1H, d, $J = 15.6$ Hz), 7.26 (1H, d, $J = 8.5$ Hz), 7.23 (1H, s), 7.11 (1H, d, $J = 8.3$ Hz), 6.90 (1H, d, $J = 8.2$ Hz), 6.45 (2H, d, $J = 8.3$ Hz). ^{13}C NMR (acetone- d_6 , 125 MHz, ppm): δ 194.5, 162.3, 148.4, 145.6, 144.1, 135.9, 127.7, 124.5, 122.6, 115.7, 114.8, 110.9, 107.8. HRMS: Calculated for $\text{C}_{15}\text{H}_{12}\text{O}_5\text{Na}$ [M^+Na] 295.0582, found 295.0591.

2.1.2.3.12. (*E*)-1-(2,5-Dihydroxyphenyl)-3-(3,4-dihydroxyphenyl)prop-2-en-1-one (**12**). Synthesized according to the MOMO protection, aldol condensation, and general MOMO deprotection procedure described above. Brown solid. Yield: 80.5%. ^1H NMR (acetone- d_6 , 500 MHz, ppm): δ 7.80 (1H, d, $J = 15.1$ Hz), 7.67 (1H, d, $J = 15.6$ Hz), 7.58 (1H, s), 7.38 (1H, s), 7.24 (1H, d, $J = 8.2$ Hz), 7.11 (1H, d, $J = 9.2$ Hz), 6.92 (1H, d, $J = 8.2$ Hz), 6.83 (1H, d, $J = 9.2$ Hz). ^{13}C NMR (acetone- d_6 , 125 MHz, ppm): δ 156.9, 149.4, 148.8, 146.0, 145.7, 127.2, 124.7, 123.0, 120.0, 118.6, 117.4, 115.7, 115.3, 114.7. HRMS: Calculated for $\text{C}_{15}\text{H}_{12}\text{O}_5\text{Na}$ [M^+Na] 295.0582, found 295.0582.

2.1.2.3.13. (*E*)-1,3-Bis(3,4-dihydroxyphenyl)prop-2-en-1-one (**13**)⁵². Synthesized according to the MOMO protection, aldol condensation, and general MOMO deprotection procedure described above. Dark red solid. Yield: 34.0%. ^1H NMR (acetone- d_6 , 500 MHz, ppm): δ 7.64–7.61 (3H, m), 7.58 (1H, s), 7.30 (1H, s), 7.16 (1H, d, $J = 8.2$ Hz), 6.94 (1H, d, $J = 8.7$ Hz), 6.88 (1H, d,

$J = 8.3$ Hz). ^{13}C NMR (acetone- d_6 , 125 MHz, ppm): δ 150.1, 148.0, 145.5, 145.2, 143.6, 131.2, 127.7, 122.1, 122.1, 119.0, 115.6, 115.4, 114.9, 114.8. HRMS: Calculated for $\text{C}_{15}\text{H}_{12}\text{O}_5\text{Na}$ [M^+Na] 295.0582, found 295.0576.

2.1.2.3.14. (*E*)-3-(3,4-Dihydroxyphenyl)-1-(3,5-dihydroxyphenyl)prop-2-en-1-one (**14**). Synthesized according to the MOMO protection, aldol condensation, and general MOMO deprotection procedure described above. Black solid. Yield: 84.0%. ^1H NMR (acetone- d_6 , 500 MHz, ppm): δ 7.62 (1H, d, $J = 15.6$ Hz), 7.43 (1H, d, $J = 15.6$ Hz), 7.30 (1H, s), 7.16 (1H, d, $J = 7.8$ Hz), 7.04 (2H, s), 6.98 (1H, d, $J = 8.2$ Hz), 6.59 (1H, s). ^{13}C NMR (acetone- d_6 , 125 MHz, ppm): δ 189.1, 171.5, 170.3, 158.9, 148.3, 145.6, 144.6, 140.9, 127.4, 122.3, 119.3, 115.6, 114.8, 106.8, 106.8. HRMS: Calculated for $\text{C}_{15}\text{H}_{12}\text{O}_5\text{Na}$ [M^+Na] 295.0582, found 295.0578.

2.1.2.3.15. (*E*)-1-(2,4-Dihydroxyphenyl)-3-(3,4-dihydroxyphenyl)prop-2-en-1-one (**15**)⁵³. Synthesized according to the MOMO protection, aldol condensation, and general MOMO deprotection procedure described above. Red solid. $R_f = 0.19$ (5% $\text{CH}_3\text{OH}/\text{CH}_2\text{Cl}_2$). Yield: 78.7%. ^1H NMR (acetone- d_6 , 500 MHz, ppm): δ 8.11 (1H, d, $J = 8.7$ Hz), 7.76 (1H, d, $J = 15.2$ Hz), 7.69 (1H, d, $J = 15.2$ Hz), 7.35 (1H, s), 7.22 (1H, d, $J = 8.3$ Hz), 6.90 (1H, d, $J = 8.2$ Hz), 6.46 (1H, d, $J = 8.8$ Hz), 6.36 (1H, s). ^{13}C NMR (acetone- d_6 , 125 MHz, ppm): δ 192.0, 166.8, 164.8, 148.4, 145.6, 144.8, 132.5, 127.4, 122.7, 117.6, 115.6, 115.2, 113.7, 107.9, 103.0. HRMS: Calculated for $\text{C}_{15}\text{H}_{12}\text{O}_5\text{Na}$ [M^+Na] 295.0582, found 295.0587.

2.1.2.3.16. (*E*)-3-(2,3-Dihydroxyphenyl)-1-(3,4-dihydroxyphenyl)prop-2-en-1-one (**16**). Synthesized according to the MOMO protection, aldol condensation, and general MOMO deprotection procedure described above. Brown solid. Yield: 57.0%. ^1H NMR (acetone- d_6 , 500 MHz, ppm): δ 8.09 (1H, d, $J = 16.1$ Hz), 7.81 (1H, d, $J = 15.6$ Hz), 7.62 (1H, s), 7.61 (1H, d, $J = 6.4$ Hz), 7.28 (1H, d, $J = 7.8$ Hz), 6.95 (1H, d, $J = 7.8$ Hz), 6.92 (1H, d, $J = 7.8$ Hz), 6.74 (1H, t, $J = 8.0$ Hz). ^{13}C NMR (acetone- d_6 , 125 MHz, ppm): δ 187.6, 151.5, 149.9, 145.6, 145.1, 138.4, 131.3, 122.5, 122.1, 121.9, 119.7, 119.6, 116.4, 115.3, 114.8. HRMS: Calculated for $\text{C}_{15}\text{H}_{11}\text{O}_5$ [$\text{M}-\text{H}$] 271.0601, found 271.0608.

2.1.2.3.17. (*E*)-3-(2,5-Dihydroxyphenyl)-1-(3,4-dihydroxyphenyl)prop-2-en-1-one (**17**). Synthesized according to the MOMO protection, aldol condensation, and general MOMO deprotection procedure described above. Black solid. Yield: 88.4%. ^1H NMR (acetone- d_6 , 500 MHz, ppm): δ 8.04 (1H, d, $J = 15.6$ Hz), 7.74 (1H, d, $J = 16.1$ Hz), 7.62 (1H, s), 7.60 (1H, d, $J = 8.3$ Hz), 7.21 (1H, s), 6.95 (1H, d, $J = 8.2$ Hz), 6.84 (1H, d, $J = 8.7$ Hz), 6.78 (1H, d, $J = 8.7$ Hz). ^{13}C NMR (acetone- d_6 , 125 MHz, ppm): δ 187.8, 150.5, 150.3, 150.0, 145.1, 138.6, 131.2, 122.7, 122.0, 121.5, 118.9, 117.0, 115.4, 115.0, 113.9. HRMS: Calculated for $\text{C}_{15}\text{H}_{11}\text{O}_5$ [$\text{M}-\text{H}$] 271.0601, found 271.0614.

2.1.2.3.18. (*E*)-3-(3,4-Dihydroxyphenyl)-1-(2,3,4-trihydroxyphenyl)prop-2-en-1-one (**18**). Synthesized according to the MOMO protection, aldol condensation, and general MOMO deprotection procedure described above. Red solid. Yield: 97.1%. ^1H NMR (acetone- d_6 , 500 MHz, ppm): δ 7.76 (1H, d, $J = 15.2$ Hz), 7.70 (1H, d, $J = 8.7$ Hz), 7.69 (1H, d, $J = 15.6$ Hz), 7.35 (1H, s), 7.23 (1H, d, $J = 8.2$ Hz), 6.90 (1H, d, $J = 8.3$ Hz), 6.50 (1H, d, $J = 8.7$ Hz). ^{13}C NMR (acetone- d_6 , 125 MHz, ppm): δ 192.5, 153.0, 151.6, 148.3, 145.4, 144.7, 132.3, 127.4, 122.7, 122.4, 117.7, 115.6, 115.2, 114.0, 107.4. HRMS: Calculated for $\text{C}_{15}\text{H}_{11}\text{O}_6$ [$\text{M}-\text{H}$] 287.0550, found 287.0557.

2.1.2.3.19. (*E*)-1-(3,4-Dihydroxyphenyl)-3-(2,3,4-trihydroxyphenyl)prop-2-en-1-one (**19**). Synthesized according to the MOMO protection, aldol condensation, and general MOMO deprotection procedure described above. Brown solid. Yield: 44.0%. ^1H NMR (D_2O , 500 MHz, ppm): δ 8.46 (1H, d, $J = 8.2$ Hz), 7.58 (1H, d, $J = 8.7$ Hz), 7.28–7.24 (m, 2H), 7.05 (1H, d, $J = 8.7$ Hz), 6.97 (1H, s), 6.46 (1H, d, $J = 8.2$ Hz). ^{13}C NMR (D_2O , 125 MHz, ppm): δ 191.2, 169.0, 168.5, 159.2, 158.3, 143.6, 137.7, 125.3, 122.5, 121.0,

117.4, 115.4, 113.8, 111.8, 110.0. HRMS: Calculated for $C_{15}H_{11}O_6$ [M–H] 287.0550, found 287.0558.

2.1.2.3.20. (*E*)-1,3-Bis(2,3,4-trihydroxyphenyl)prop-2-en-1-one (**20**). Synthesized according to the MOMO protection, aldol condensation, and general MOMO deprotection procedure described above. Brown solid. Yield: 95.7%. 1H NMR (acetone- d_6 , 500 MHz, ppm): δ 8.19 (1H, d, $J = 15.6$ Hz), 7.83 (1H, d, $J = 15.6$ Hz), 7.60 (1H, d, $J = 9.2$ Hz), 7.24 (1H, d, $J = 8.7$ Hz), 6.50 (2H, d, $J = 9.2$ Hz). ^{13}C NMR (acetone- d_6 , 125 MHz, ppm): δ 192.9, 153.0, 151.3, 148.4, 147.3, 140.6, 132.5, 132.3, 122.0, 121.0, 117.4, 115.0, 114.1, 107.9, 107.3. HRMS: Calculated for $C_{15}H_{11}O_7$ [M–H] 303.0499, found 303.0509.

2.2. Activity assays

2.2.1. Materials for bioassays

Bovine XO, xanthine, potassium phosphate, the 2,2-diphenyl-1-picrylhydrazyl (DPPH) radical, and 3-(4,5-dimethylthiazol-2-yl)-2,5-diphenyltetrazolium bromide (MTT) were received from Sigma/Aldrich. Dimethylformamide (DMF), and phosphate-buffered saline (PBS) were purchased from Fisher Scientific. Murine Neuro-2A cells were received from Eton Bioscience (San Diego, CA) whereas growth medium, serum, trypsin, and antibiotics were obtained from Atlanta Biologicals (Atlanta, GA). A β 25–35 was from Abbiotec (San Diego, CA).

2.2.2. Determination of inhibitory potency against XO activity

The rate of XO-catalyzed conversion of xanthine to uric acid was determined spectroscopically by measuring the concomitant absorbance change at 295 nm for five min.⁷ XO (0.1 units/mg) was suspended in buffer (20 mM phosphate, pH 7.5) and the reaction was triggered by adding the enzyme buffer (final XO concentration: 39 μ g/mL) to xanthine dissolved in the same buffer (final concentration: 46 μ M; total volume: 200 μ L), using 96-well plastic plates capable of transmitting UV light that were placed in a microplate reader (SpectraMax 190, Molecular Devices, Sunnyvale, CA). Assays were conducted in the absence and presence of potential inhibitors at 11 different concentrations. The exact inhibitor concentrations used in the assay depended on the potency of the test compound and were chosen so that the IC_{50} value was located approximately in the center of the concentration range. Reaction rates were obtained by linear regression of the absorbance versus time traces and then fit to a three-parameter logistic equation. Inhibitory potencies were expressed as IC_{50} values,⁵⁴ the inhibitory concentrations that reduced XO activity by 50%.

2.2.3. Measurement of DPPH scavenging activity

The abilities of compounds to scavenge the stable radical DPPH were measured by mixing 50 μ L of a freshly prepared solution of DPPH in ethanol (0.2 mM) with 150 μ L of the test compound in ethanol at several concentrations ranging from 5 to 50 μ M.⁵⁵ Samples were placed in a 96-well plate and incubated for 30 min at room temperature in the dark. The disappearance of the DPPH absorbance at a wavelength of 517 nm, an indicator of radical scavenging, was measured with a plate reader.

2.2.4. Assessment of cell viability in the presence of A β

The ability of chalcones to improve the viability of cells exposed to cytotoxic A β was assessed according to an established protocol using Neuro-2A neuroblastoma cells.^{19,20} According to previous work, exposure to self-aggregating β -amyloid peptide induces elevated levels of ROS via activation of NADPH oxidase.⁵⁶ Cells were grown according to the supplier's guidelines in Dulbecco's minimum essential medium complemented with 10% of fetal bovine

serum and 100 units/mL penicillin–streptomycin at 37 °C in an atmosphere of 95% air and 5% carbon dioxide. For seeding, cells were washed with PBS, treated with trypsin for no longer than one minute, and then placed in 100 μ L aliquots in a 96-well plate at a density of 2000–4000 cells/mL. After 6 h of incubation, a 10 μ L aliquot of 250 μ M test compound, 15 μ L of 833 μ M A β , and 25 μ L of MTT buffer (5 mg/mL in PBS) were added to each well.⁵⁷ After six hours of incubation, 100 μ L of extraction buffer (prepared by addition of 2.5% v/v of a mixture composed of four parts of acetic acid and one part of 20% w/v SDS prepared in a 50:50 mix of DMF and water, pH 4.7) was added. After 6 h on an incubating shaker (25 rpm) in the dark at 37 °C, the absorbances of the samples were measured at 570 nm with a microplate reader.

2.3. Computation of inhibitor binding poses by computational ligand docking

Inhibitor structures of **8**, **9**, **15**, **16**, and **20** were modeled in MOE (version 2013.08; Chemical Computing Group, Montreal, Canada) and energy-minimized using the MMFF94s force field. All minimization parameters were kept at their default settings, except for the dielectric constant, which was set to a value of 4 to account for the relatively hydrophobic character of the protein interior. Docking of chalcones was performed with the program GOLD (version 5.2; Cambridge Crystallographic Data Centre, UK)^{58,59} using the X-ray crystal structure of the XO/xanthine complex (Protein Data Bank entry 3EUB).⁶⁰ The protein structure was prepared in GOLD for docking by adding hydrogen atoms and deleting xanthine. All other non-protein entities such as prosthetic groups remained unchanged. The scoring function selected for docking was ChemScore^{61,62} and the genetic algorithm of GOLD was executed at the default settings, performing 30 independent and identical repeats. The docking site was defined as the area occupied by the deleted xanthine ligand plus a 6 Å wide zone in its immediate proximity, yielding a docking area that was large enough to accommodate each of the docked chalcones.

3. Results and discussion

3.1. Synthesis of chalcones

Simple mono-substituted chalcones were successfully prepared through the Claisen–Schmidt condensation of the corresponding acetophenones and benzaldehydes (compounds **1–5**). For the synthesis of di-, tri-, tetra-, penta-, and hexasubstituted chalcones, a three-step route was utilized (Fig. 2). More specifically, the hydroxyl groups in aldehydes or acetophenones were protected by MOMO groups under basic reflux conditions.⁶³ Claisen–Schmidt condensation of these protected aldehydes and acetophenones provided enones.^{64,65} In the case of mono-, di-, or tri-substituted chalcones, the corresponding enone products mostly precipitated after acidic workup. These enones were then filtered and further purified by recrystallization. In the cases of tetra-, penta-, and hexasubstituted chalcones, the enone products did not precipitate and an acid/base extraction was utilized instead to obtain crude products. Enone compounds were treated with 10% HCl to remove the MOMO protecting groups⁶⁶ and yield the chalcone compounds (Fig. 1, compounds **6–20**). The chalcones with four or more hydroxyl groups showed poor solubility in organic solvents. Their solubility in water was pH-dependent, with poor solubility at low pH and high solubility at high pH. 1H NMR spectra revealed that the coupling constants of the two olefinic protons were around 16 Hz, indicating the *E* configuration of the olefinic bond in these chalcones. All synthesized compounds were fully characterized by 1H NMR and ^{13}C NMR spectroscopy and by HRMS.

3.2. Inhibition of XO activity by chalcones

Among the 20 tested chalcones (see Fig. 3 for a representative result), 15 displayed measurable inhibitory potencies (Table 1 and Fig. 1), with IC_{50} values ranging from 1.2 (**18**) to 290 μ M (**5**). Inspection of the chemical structures of the active chalcones showed a general requirement for three or more hydroxyl groups for good potency, with compounds **18** and **15** being the most potent inhibitors in the test pool (IC_{50} values of 1.2 and 1.3 μ M, respectively). As the comparison of the potencies of **7** and **9** and of **8** and **13** revealed, the presence of hydroxyl groups in position 4' of the A-ring increased a compound's potency. A similar trend was observed for position 3', where an additional hydroxyl group rendered chalcones more active (**9** vs **13** and **7** vs **8**). Findings pertaining to position 2' were more ambiguous, as evident from a potency increase seen for **9** versus **15** and for **13** versus **18**, but a decrease observed for **8** versus **12**.

Structural variations in the B-ring were more limited, but an increase in potency was noted by the introduction of a hydroxyl group in positions 3 (**6** vs **10**) and 4 (**16** vs **19**). In contrast, an additional hydroxyl group in position 2 was detrimental to potency (**13** vs **19** and **18** vs **20**).

3.3. Computational prediction of chalcone binding to XO

Despite the availability of a relatively large number of high resolution X-ray crystal structures of bovine XO in complex with various small molecules,^{16,60,67–69} no structural information exists for the binding of chalcones, leaving the molecular details of interactions between this inhibitor class and XO ambiguous. In the absence of crystallographic information, computational tools like ligand docking can provide valuable insights into critical enzyme/inhibitor interactions.⁷⁰ Among numerous commercial and academic docking routines, the program GOLD is known for its reliability and accuracy, which was the main reason for employing it for the investigation of chalcone binding to XO.^{59,71}

Docking was limited to a representative subset of high potency inhibitors (**8**, **9**, **15**, **16**, and **20**) since their interactions with the enzyme were presumably strong and therefore most likely predicted accurately by GOLD. For simplicity, initial docking focused on compounds **8** and **9** since their three hydroxyl groups represented the minimum structural requirement for high potency inhibition. Docking yielded consensus orientations, implying that the majority of independent repeats of the docking protocol generated identical solutions (21/30 for **8** and 17/30 for **9**). Control docking

Table 1

Experimentally determined inhibitory potencies, radical scavenging activities, and cell viability data for the 20 chalcones

Compound #	IC_{50}/μ M	% DPPH scavenging	% cell viability
1	Inactive	6.7 \pm 5	1.7 \pm 1
2	Inactive	0.2 \pm 4	5.9 \pm 5
3	Inactive	–1.4 \pm 3	1.4 \pm 2
4	Inactive	–0.6 \pm 4	3.0 \pm 4
5	290 \pm 40	–9.1 \pm 10	0
6	Inactive	–3.0 \pm 1	3.9 \pm 8
7	53 \pm 20	90 \pm 1	4.3 \pm 6
8	5.3 \pm 1	82 \pm 9	35 \pm 6
9	4.3 \pm 1	42 \pm 3	28 \pm 6
10	27 \pm 20	0.5 \pm 2	6.9 \pm 7
11	35 \pm 10	90 \pm 9	28 \pm 2
12	17 \pm 8	91 \pm 1	46 \pm 6
13	3.0 \pm 0.6	77 \pm 20	40 \pm 2
14	6.5 \pm 2	84 \pm 3	26 \pm 3
15	1.3 \pm 0.4	90 \pm 2	71 \pm 2
16	93 \pm 30	70 \pm 10	46 \pm 2
17	8.6 \pm 2	86 \pm 1	70 \pm 5
18	1.2 \pm 0.2	92 \pm 3	118 \pm 7
19	18 \pm 3	57 \pm 2	51 \pm 3
20	5.5 \pm 0.9	82 \pm 1	91 \pm 6

Entries are the averages and standard deviations of at least three independent trials.

runs for **8** with a larger binding site (8 Å instead of 6 Å) resulted in virtually the same results but required longer computation times, which is why the smaller site was used for all subsequent runs. As shown in Figure 4 (middle panel), the two hydroxyl groups on the B ring of **8** formed hydrogen bonds with the side chain carboxyl groups of Glu802 and Glu1261 whereas the carbonyl oxygen was engaged with the hydroxyl groups of Ser876. The docking results for **15**, **16**, and **20** were more diverse, but all contained predicted poses that overlapped with those seen for **8** and **9**, which were used for further analysis (Fig. 4, upper panel). The XO side chains involved in binding of **15** and **16** were the same as for **8** and **9**, whereas **20**, the only compound with six hydroxyl groups, was predicted to form additional, albeit weaker hydrogen bonds to Thr1010 and Arg880. A second major driving force to inhibitor binding came from hydrophobic interactions, which exceeded the energetic contributions of hydrogen bonding by a factor of about three for all compounds docked. In comparison to the binding site entrance, the walls and the bottom of the cavity are more hydrophobic (Fig. 4, lower panel), allowing for favorable hydrophobic interactions of an inhibitor's B-ring and the carbon–carbon double bond with nonpolar side chains (Phe941, Phe1009, Phe1013, Leu648, Leu873, Val1011, Ala910, Ala1078, Ala1079, and Pro1076). Contributions to the docking score arising from factors other than hydrogen bonding and hydrophobic interactions, such as unfavorable energy terms due to steric clashes and the loss of conformational freedom upon ligand binding, were minor and could therefore be safely omitted.

3.4. DPPH radical scavenging by chalcones

Among the twenty tested chalcones, thirteen were capable of scavenging the DPPH radical to a noticeable degree. The ability to reduce the stable DPPH radical is a frequently considered measure for a compound's potential to scavenge long-lived radicals. In a typical experiment, DPPH was incubated with the test compound at several concentrations up to 100 μ M for 30 min. The DPPH absorbance was then and converted into radical scavenging activity according to:

$$\text{Activity} = \left(1 - \frac{A_{\text{test}}}{A_{\text{control}}}\right) 100\%$$

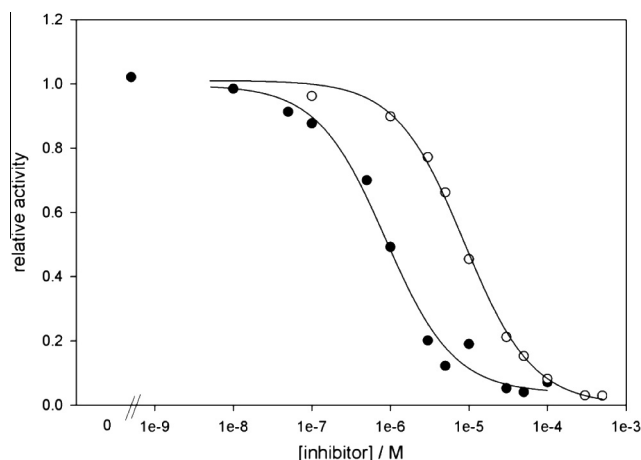


Figure 3. Representative XO activity inhibition assay for compounds **12**(○) and **15** (●). The lines represent fits of a three-parameter logistic curve to the data points.

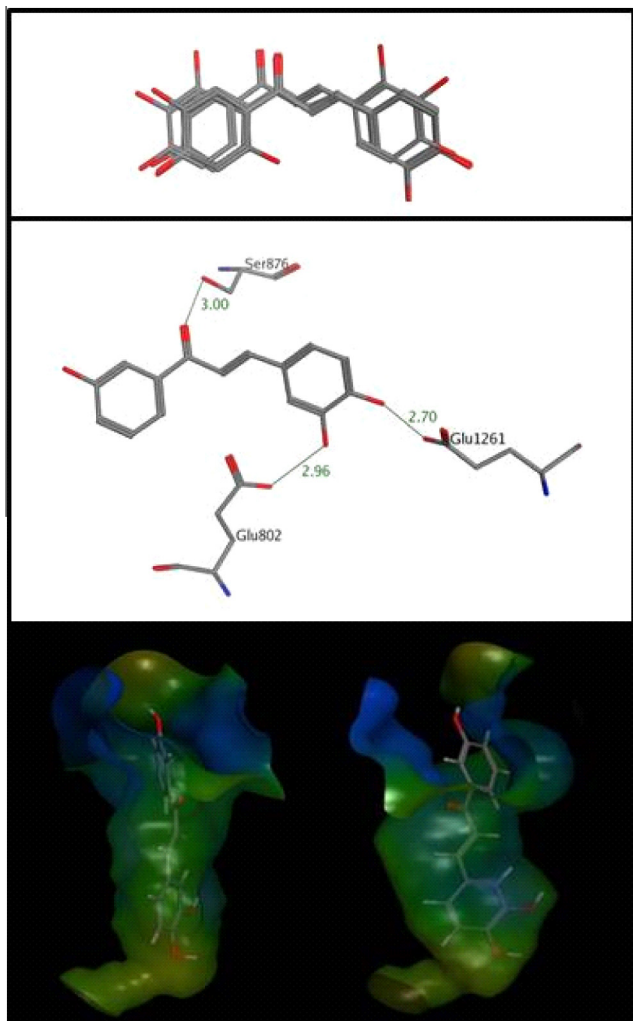


Figure 4. Docking-predicted poses of chalcones in the XO binding site. Upper panel: consensus binding poses of chalcones **8**, **9**, **15**, **16**, and **20**. Middle panel: predicted hydrogen bond interactions (thin grey lines) between **8** and the XO binding site. Lower panel: front and side views of **8** in the binding site with a hydrophobic index map superimposed on the binding site of XO (colors in decreasing hydrophobicity: brown–green–blue).

The control sample was devoid of a scavenger and reported activities were obtained at a chalcone concentration of 20 μM (Fig. 5 and Table 1).

Inspection of the DPPH radical scavenging abilities revealed that the chalcones could be clearly divided into two groups with unique behavior. They either had clearly detectable activities varying from 39 to 92% (**7–9** and **11–20**) or were essentially inactive (all other compounds). Some chalcones exceeded the scavenging ability of the known antioxidant ascorbic acid noticeably (Fig. 5). The obvious structural feature that all active compounds shared was the presence of two hydroxyl groups located at neighboring carbon atoms at one or both phenyl rings of the chalcone scaffold. This observation was in agreement with the results of a study on phenolic compounds that showed that two hydroxyl groups in 1,2 or 1,4 positions were optimal for radical scavenging activity. The observed behavior was accounted for using resonance structures showing increased stabilization of a formed radical by a second, electron-donating hydroxyl group in the indicated positions.⁷² Moreover, a comparison of the standard reduction potentials of catechol (530 mV), resorcinol (720 mV), and hydroquinone (459 mV) shows the higher likelihood of 1,2- and 1,4-dihydroxybenzenes to become oxidized.⁷³

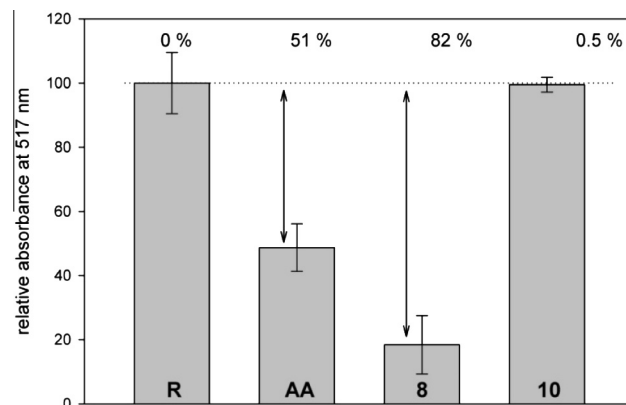


Figure 5. Representative DPPH radical scavenging assay. Bar heights indicate the amount of DPPH radical remaining in a sample after incubation with a potential scavenger. The first bar (**R**) represents a reference conducted in the absence of test compounds whereas the next three bars depict samples in the presence of the known scavenger ascorbic acid (**AA**), compound **8**, and compound **10** (all at 20 μM). The arrows indicate the percentage of DPPH scavenged by the test compound, calculated as described under Section 2.

3.5. Ability of chalcones to protect cells from A β -induced cytotoxicity

To be of use for therapeutic purposes, compounds need to be able to suppress ROS-related stress in living cells. As most of the chalcones in this study were capable of inhibiting XO and/or scavenging the DPPH radical, we evaluated their ability to rescue cells with elevated ROS-levels. As a simple model for the evaluation of chalcones under *in situ* conditions, they were added to cultured Neuro-2A cells that had been exposed to A β , an agent known to activate NADPH oxidase and thereby generate ROS.⁵⁶ Neurons were chosen as a model since they are a potential target of stroke-induced reperfusion injuries. A MTT-based cell viability assay permitted the study of the effect of the added chalcones on cell survival rates. Cell viability percentages (Table 1) were obtained by dividing the MTT absorbance at 570 nm by the absorbance of a control sample not subjected to ROS-induced stress (Fig. 6).

The results summarized in Table 1 showed that compounds offering the best level of protection were those with dual activities (**15**, **17**, **18**, and **20**), that is, good DPPH scavengers (>80% scavenging activity) with high inhibitory potencies against XO activity ($\text{IC}_{50} < 10 \mu\text{M}$). The only exception to this trend was **8**, which offered only modest protection against ROS-induced stress. Interestingly, **8** was the only compound with dual activities that possessed three hydroxyl groups, whereas **15**, **17**, **18**, and **20** had between four and six hydroxyl groups and were therefore more polar. It is conceivable that the difference in polarity and hydrophobicity caused the protective ability of **8** to differ from those of the chalcones mentioned above since in living cells properties such as cell permeability or solubility are known to affect a compound's bioactivity. A few other chalcones, among them **9**, **11**, **12**, **13**, **14**, **16**, and **19** increased cell viability at a modest but noticeable level. As an inspection of their activities revealed, these compounds were either good inhibitors or good DPPH scavengers, but not both. It should be noted that none of the mono- or di-hydroxylated chalcones increased cell viability, reemphasizing the need for multiple hydroxyl groups to be useful for enhancing the viability of cells exposed to ROS-induced stress. Overall, the findings indicated that the best protection of neurons was afforded by poly-hydroxylated chalcones that combined high inhibitory potencies with good radical scavenging abilities within the same molecule.

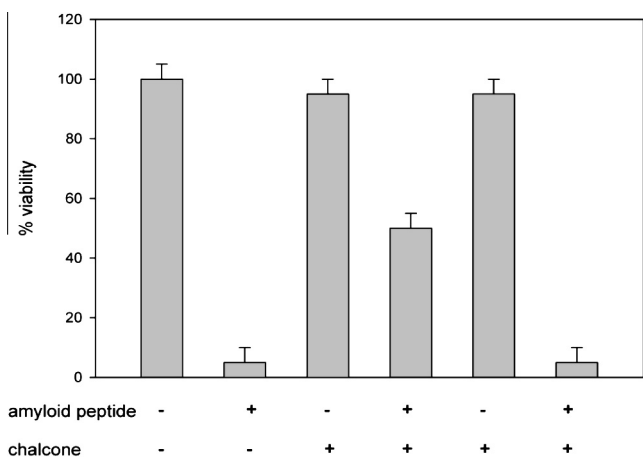


Figure 6. Representative results of a cell viability assay under A β -induced cytotoxicity for compounds **10** and **12**. Bar heights correspond directly to the absorbance of the dye MTT at 570 nm, a direct measure for viability of Neuro 2A cells. The first two bars represent control measurements in the absence of chalcones in the absence and presence of A β , respectively. The third and fourth bars represent measurements for compound **12**, which exhibited good rescue properties. Bars five and six were obtained for compound **10**, a poor rescue compound.

Whereas the findings were compatible with a mechanism of action that relied on XO inhibition and radical scavenging to reduce ROS levels, they certainly did not provide ultimate proof for such a scenario because of the complexity of a living cell in comparison to in vitro assays. Other mechanisms of cell protection unrelated to XO inhibition or radical scavenging may also have been involved. In addition to physical properties influencing bioavailability, such possibilities include but are not limited to anti-inflammatory or epigenetic effects and modification of metallo-enzymes, cofactors, or gene expression levels.

3.6. Conclusions

In this study, we demonstrated that Claisen–Schmidt condensation is a convenient and effective synthetic route that provides access to a variety of chalcones. In addition, the bioassays performed with synthesized chalcones represent the first systematic assessment of these compounds' abilities to inhibit XO and scavenge the stable radical DPPH. SARs derived from in vitro assays showed that a minimum of three hydroxyl groups was a requirement of effective XO inhibition. The DPPH radical scavenging assays indicated that two hydroxyl groups at neighboring positions on at least one phenyl ring were a prerequisite for good scavenging activity. Subsequent cell viability assays with neurons subjected to ROS-induced stress supported the hypothesis that chalcones that combined both properties in a single molecule offered the best protection, suggesting that these compounds may bear the potential eventually of becoming a novel type of drugs against ROS-induced stress that could, for example, be used for the prevention of reperfusion injuries. However, additional work is needed to further modify the structure of the chalcone scaffold to optimize inhibitory and scavenging properties. In addition, assays need to be performed that monitor scavenging of radicals of direct physiological relevance, such as the superoxide anion or the hydroxyl radical.

Acknowledgements

This work was supported in part by grants from the National Institutes of Health (Institutional Development Award 5P20GM103436 to S.P. and L.M. and Academic Research Enhancement Award 1R15GM084431-02 to S.P.). Support from

National Science Foundation award 1040302 for mass spectrometry is also acknowledged.

References and notes

- Veitch, N. C.; Grayer, R. J. *Chalcones, Dihydrochalcones, and Aurones. In Flavonoids. Chemistry, Biochemistry and Applications*; Andersen, Ø. M., Markham, K. R., Eds.; CRC Press, 2005; pp 1003–1100.
- Ameta, K. L.; Gupta, V. K.; Gaur, R. *The Biochemistry of Chalcones: Chalcones: Synthesis and Biological Evaluation*; Lap Lambert Academic Publishing, 2011.
- Batovska, D. I.; Todorova, I. T. *Curr. Clin. Pharmacol.* **2010**, *5*, 1.
- Dimmock, J. R.; Elias, D. W.; Beazely, M. A.; Kandepu, N. M. *Curr. Med. Chem.* **1999**, *6*, 1125.
- Singh, P.; Anand, A.; Kumar, V. *Eur. J. Med. Chem.* **2014**, *85C*, 758.
- Pacher, P.; Nivorozhkin, A.; Szabo, C. *Pharmacol. Rev.* **2006**, *58*, 87.
- Borges, F.; Fernandes, E.; Roleira, F. *Curr. Med. Chem.* **2002**, *9*, 195.
- Hak, A. E.; Choi, H. K. *Curr. Opin. Rheumatol.* **2008**, *20*, 179.
- Dalbeth, N.; Stamp, L. *Semin. Dial.* **2007**, *20*, 391.
- Singer, J. Z.; Wallace, S. L. *Arthritis Rheum.* **1986**, *29*, 82.
- Arellano, F.; Sacristan, J. A. *Ann. Pharmacother.* **1993**, *27*, 337.
- Stamp, L. K. *Curr. Opin. Rheumatol.* **2014**, *26*, 162.
- Terkeltaub, R.; Bushinsky, D. A.; Becker, M. A. *Arthritis Res. Ther.* **2006**, *8*, S4.
- Burns, C. M.; Wortmann, R. L. *Lancet* **2011**, *377*, 165.
- Diaz-Torne, C.; Perez-Herrero, N.; Perez-Ruiz, F. *Curr. Opin. Rheumatol.* **2015**, *27*, 164.
- Okamoto, K.; Eger, B. T.; Nishino, T.; Kondo, S.; Pai, E. F.; Nishino, T. *J. Biol. Chem.* **2003**, *278*, 1848.
- Garcia-Valladares, I.; Khan, T.; Espinoza, L. R. *Ther. Adv. Musculoskelet. Dis.* **2011**, *3*, 245.
- Stamp, L. K.; O'Donnell, J. L.; Chapman, P. T. *Int. Med. J.* **2007**, *37*, 258.
- Chang, Y. C.; Lee, F. W.; Chen, C. S.; Huang, S. T.; Tsai, S. H.; Huang, S. H.; Lin, C. M. *Free Radic. Biol. Med.* **2007**, *43*, 1541.
- Lin, H. C.; Tsai, S. H.; Chen, C. S.; Chang, Y. C.; Lee, C. M.; Lai, Z. Y.; Lin, C. M. *Biochem. Pharmacol.* **2008**, *75*, 1416.
- Hofmann, E.; Webster, J.; Kidd, T.; Kline, R.; Jayasinghe, M.; Paula, S. *Int. J. Biosci., Biochem. Bioinform.* **2014**, *4*, 5.
- Bayir, H. *Crit. Care Med.* **2005**, *33*, S498.
- Halliwell, B. *J. Neurochem.* **2006**, *97*, 1634.
- Halliwell, B. *Biochem. J.* **2007**, *401*, 1.
- Zweier, J. L.; Talukder, M. A. *Cardiovasc. Res.* **2006**, *70*, 181.
- Gorrini, C.; Harris, I. S.; Mak, T. W. *Nat. Rev. Drug Disc.* **2013**, *12*, 931.
- Dorion, D.; Zhong, A.; Chiu, C.; Forrest, C. R.; Boyd, B.; Pang, C. Y. *J. Appl. Physiol.* **1993**, *75*, 246.
- McCord, J. M. *N. Engl. J. Med.* **1985**, *312*, 159.
- Khalil, A. A.; Aziz, F. A.; Hall, J. C. *Plast. Reconstr. Surg.* **2006**, *117*, 1024.
- Kalogeris, T.; Baines, C. P.; Krenz, M.; Korthuis, R. J. *Int. Rev. Cell Mol. Biol.* **2012**, *298*, 229.
- Cheng, Z. J.; Kuo, S. C.; Chan, S. C.; Ko, F. N.; Teng, C. M. *Biochim. Biophys. Acta* **1998**, *1392*, 291.
- Haraguchi, H.; Ishikawa, H.; Mizutani, K.; Tamura, Y.; Kinoshita, T. *Bioorg. Med. Chem.* **1998**, *6*, 339.
- Kong, L. D.; Zhang, Y.; Pan, X.; Tan, R. X.; Cheng, C. H. *Cell Mol. Life Sci.* **2000**, *57*, 500.
- Schempp, H.; Vogel, S.; Huckelhoven, R.; Heilmann, J. *Free Radic. Res.* **2010**, *44*, 1435.
- Tung, Y. T.; Hsu, C. A.; Chen, C. S.; Yang, S. C.; Huang, C. C.; Chang, S. T. *J. Agric. Food Chem.* **2010**, *58*, 9936.
- Chang, W. S.; Chiang, H. C. *Anticancer Res.* **1995**, *15*, 1969.
- Ozer, M. K.; Parlakpinar, H.; Acet, A. *Clin. Biochem.* **2004**, *37*, 702.
- Irmak, M. K.; Fadillioglu, E.; Sogut, S.; Erdogan, H.; Gulec, M.; Ozer, M.; Yagmurca, M.; Gozukara, M. E. *Cell Biochem. Funct.* **2003**, *21*, 283.
- Ozyurt, B.; Iraz, M.; Koca, K.; Ozyurt, H.; Sahin, S. *Mol. Cell. Biochem.* **2006**, *292*, 197.
- Krishnakumar, B.; Velmurugan, R.; Swaminathan, M. *Catal. Commun.* **2011**, *12*, 375.
- Sultan, A.; Raza, A. R.; Abbas, M.; Khan, K. M.; Tahir, M. N.; Saari, N. *Molecules* **2013**, *18*, 10081.
- Sutradhar, N.; Sinhamahapatra, A.; Pahari, S. K.; Pal, P.; Bajaj, H. C.; Mukhopadhyay, I.; Panda, A. B. *J. Phys. Chem. C* **2011**, *115*, 12308.
- Shakil, N. A.; Singh, M. K.; Sathiyendiran, M.; Kumar, J.; Padaria, J. C. *Eur. J. Med. Chem.* **2013**, *59*, 120.
- Lahyani, A.; Chtourou, M.; Frikha, M. H.; Trabelsi, M. *Ultrason. Sonochem.* **2013**, *20*, 1296.
- Moriyama, K.; Takemura, M.; Togo, H. *J. Org. Chem.* **2014**, *79*, 6094.
- Garcia-Alvarez, J.; Diez, J.; Vidal, C.; Vicent, C. *Inorg. Chem.* **2013**, *52*, 6533.
- Schranck, J.; Wu, X. F.; Neumann, H.; Beller, M. *Chem. Eur. J.* **2012**, *18*, 4827.
- Cardona, F.; Rocha, J.; Silva, A. M. S.; Guieu, S. *Dyes Pigments* **2014**, *111*, 16.
- Silva, W. A.; Andrade, C. K. Z.; Napolitano, H. B.; Vencato, I.; Lariucci, C.; de Castro, M. R. C.; Camargo, A. J. *Brazil. Chem. Soc.* **2013**, *24*, 133.
- Liu, H. R.; Liu, X. J.; Fan, H. Q.; Tang, J. J.; Gao, X. H.; Liu, W. K. *Bioorg. Med. Chem.* **2014**, *22*, 6124.
- Karki, R.; Thapa, P.; Kang, M. J.; Jeong, T. C.; Nam, J. M.; Kim, H.-L.; Na, Y.; Cho, W.-J.; Kwon, Y.; Lee, E.-S. *Bioorg. Med. Chem.* **2010**, *18*, 3066.
- Jun, N.; Hong, G.; Jun, K. *Bioorg. Med. Chem.* **2007**, *15*, 2396.
- Ma, L.; Yang, Z.; Li, C.; Zhu, Z.; Shen, X.; Hu, L. *J. Enzyme Inhib.* **2011**, *26*, 643.

54. Cheng, Y.; Prusoff, W. H. *Biochem. Pharmacol.* **1973**, *22*, 3099.
55. Sharma, O. P.; Bhat, T. K. *Food Chem.* **2009**, *113*, 1202.
56. Abramov, A. Y.; Canevari, L.; Duchon, M. R. *J. Neurosci.* **2004**, *24*, 565.
57. Hansen, M. B.; Nielsen, S. E.; Berg, K. *J. Immunol. Methods* **1989**, *119*, 203.
58. Jones, G.; Willett, P.; Glen, R. C. *J. Mol. Biol.* **1995**, *245*, 43.
59. Jones, G.; Willett, P.; Glen, R. C.; Leach, A. R.; Taylor, R. *J. Mol. Biol.* **1997**, *267*, 727.
60. Pauff, J. M.; Cao, H.; Hille, R. *J. Mol. Biol.* **2009**, *284*, 8760.
61. Baxter, C. A.; Murray, C. W.; Clark, D. E.; Westhead, D. R.; Eldridge, M. D. *Proteins* **1998**, *33*, 367.
62. Eldridge, M. D.; Murray, C. W.; Auton, T. R.; Paolini, G. V.; Mee, R. P. *J. Comput. Aided Mol. Des.* **1997**, *11*, 425.
63. Jung, S. H.; Park, S. Y.; Kim-pak, Y.; Lee, H. K.; Park, K. S.; Shin, K. H.; Ohuchi, K.; Shin, H.-K.; Keum, S. R.; Lim, S. S. *Chem. Pharm. Bull.* **2006**, *54*, 368.
64. Srinivasan, B.; Johnson, T. E.; Lad, R.; Xing, C. *J. Med. Chem.* **2009**, *52*, 7228.
65. Karki, R.; Thapa, P.; Kang, M. J.; Jeong, T. C.; Nam, J. M.; Kim, H. L.; Na, Y.; Cho, W. J.; Kwon, Y.; Lee, E. S. *Bioorg. Med. Chem.* **2010**, *18*, 3066.
66. Detsi, A.; Majdalani, M.; Kontogiorgis, C. A.; Hadjipavlou-Litina, D.; Kefalas, P. *Bioorg. Med. Chem.* **2009**, *17*, 8073.
67. Enroth, C.; Eger, B. T.; Okamoto, K.; Nishino, T.; Nishino, T.; Pai, E. F. *Proc. Natl. Acad. Sci. U.S.A.* **2000**, *97*, 10723.
68. Pauff, J. M.; Zhang, J.; Bell, C. E.; Hille, R. *J. Biol. Chem.* **2008**, *283*, 4818.
69. Cao, H.; Pauff, J. M.; Hille, R. *J. Biol. Chem.* **2010**, *285*, 28044.
70. Taylor, R. D.; Jewsbury, P. J.; Essex, J. W. *J. Comput. Aided Mol. Des.* **2002**, *16*, 151.
71. Jones, G.; Willett, P.; Glen, R. C. *J. Comput. Aided Mol. Des.* **1995**, *9*, 532.
72. Ali, H.; Abo-Shady, A.; Eldeen, H.; Soror, H.; Shousha, W.; Abdel-Barry, O.; Saleh, A. *Chem. Cent. J.* **2013**, *7*, 9.
73. Steenken, S.; Neta, P. *J. Phys. Chem.* **1979**, *83*, 1134.